**AALBORG
UNIVERSITY**

Revised Rules for Concrete Bridges

Thoft-Christensen, Palle; Jensen, F. M.; Middleton, C.; Blackmore, A.

[Link to publication from Aalborg University](#)

INSTITUTTET FOR BYGNINGSTEKNIK
DEPT. OF BUILDING TECHNOLOGY AND STRUCTURAL ENGINEERING
AALBORG UNIVERSITET • AAU • AALBORG • DANMARK

P. Thoft-Christensen, F.M. Jensen, C. Middleton, A. Blackmore
REVISED RULES FOR CONCRETE BRIDGES

Revised Rules for Concrete Bridges

P. Thoft-Christensen, Aalborg University, Aalborg, Denmark
F. M. Jensen, CSRconsult, Aalborg, Denmark
C. Middleton, University of Cambridge, Cambridge, UK
A. Blackmore, University of Cambridge, Cambridge, UK

1. Introduction

This paper is based on research performed for the Highways Agency, London, UK under the project DPU/9/44 *"Revision of Bridge Assessment Rules Based on Whole Life Performance: Concrete Bridges"*. It contains details of a methodology which can be used to generate Whole Life (WL) reliability profiles. These WL reliability profiles may be used to establish revised rules for Concrete Bridges. The paper is to some extend based on Thoft-Christensen et. al. [1] and Thoft-Christensen [2].

2. Limit states

Four limit states are selected for the reliability analysis:

- two ultimate limit state (ULS):
    collapse limit state (using yield line analysis) shear failure limit state,
- a serviceability limit state (SLS):
    crack width limit state deflection limit state.

2.1 Collapse (Yield Line) Limit State
The following safety margin is used

$$Z = V E_D - W_D \tag{1}$$

where V is a model uncertainty variable, E_D is the energy dissipated in yield lines, and W_D is the work done by the applied loads.

The plastic collapse analysis and estimation of the load are performed using the COBRAS program, see Middleton [3]. The reliability analysis (element and system) is done using programs RELIAB01 and RELIAB02, see [4,5]. The RELIAB and COBRAS programs have been interfaced and include an optimisation algorithm to determine the optimal yield line pattern for each iteration of the reliability analysis, see also Thoft-Christensen [6]. The estimation of the deterioration of the steel reinforcement is based on the program CORROSION, see [7].

The basic variables used in the yield line ULS are: thickness of slab, cube strength of concrete, density of concrete, depth of reinforcement, yield strength of reinforcement, and two load parameters.

Cobras supports 16 different types of failure mode, 7 are applicable to bridge slab analysis, see figure 1.
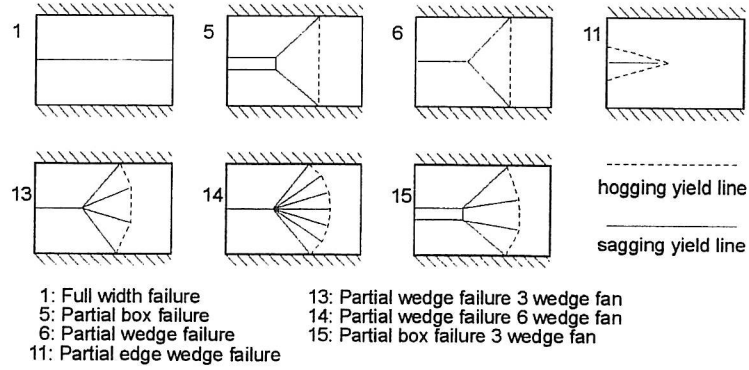
1: Full width failure	13: Partial wedge failure 3 wedge fan
5: Partial box failure	14: Partial wedge failure 6 wedge fan
6: Partial wedge failure	15: Partial box failure 3 wedge fan
11: Partial edge wedge failure	

Figure 1. Failure modes for simply supported slab bridges.

2.2 Shear Failure Limit State

Shear failure is modelled using a model applicable to reinforced concrete beams (see [8]) which may be written as

$$M_2: \quad g_2(\cdot) = Z_2 V_{j,ult} - V_j \tag{2}$$

where V_j is the shear force from external loads, $V_{j,ult}$ is the ultimate shear strength, v_c is the design shear stress, and ξ_s is the depth factor defined as, where b is the width of the beam and d is the depth of the beam

$$V_u = \xi_s v_c b d \quad , \quad v_c = 0.24 \left(\frac{100 A_s}{bd}\right)^{1/3} f_c^{1/3} \quad , \quad \xi_s = \left(\frac{500}{d}\right)^{1/4} \tag{3}$$

The stochastic variables used in the shear limit state are: thickness of slab, cover on reinforcement, concrete cube strength, yield stress of reinforcement, initial area of the reinforcement, density of concrete, static load factor, dynamic load factor, model uncertainty variable, and variables related to the chloride induced corrosion.

2.3 Crack Width Limit State

Cracking shall be limited to a level that will not impair the proper functioning of the structure or cause its appearance to be unacceptable. In the absence of specific requirements (e.g. water tightness), it may be assumed that limitation of the maximum design crack width to about 0.3 will generally be satisfactory for reinforced concrete members with respect to appearance and durability.

The design crack width may be obtained from (see [9])

$$w_k = \beta s_{rm} \varepsilon_{sm} \tag{4}$$

where w_k is the design crack width, s_{rm} is the average final spacing, ε_{sm} is the mean strain allowing, under the relevant combination of loads, for the effects of tension stiffening, shrinkage, etc., and β is a coefficient relating the average crack width to the design value. For load induced cracking $\beta = 1.7$. The value of ε_{sm} may be calculated from

$$\varepsilon_{sm} = \frac{\sigma_s}{E_s}\left[1 - \beta_1\beta_2\left(\frac{\sigma_{sr}}{\sigma_s}\right)^2\right]$$

(5)

where σ_s is the stress in the reinforcement calculated on the basis of a cracked section. σ_{sr} is the stress in the reinforcement calculated on the basis of a cracked section under the loading conditions. causing first cracking. β_1 is a coefficient which takes account of the bond properties of the bars. It is = 1.0 for high bond bars, and = 0.5 for plain bars. β_2 is a coefficient which takes account of the duration of the loading or of repeated loading. It is = 1.0 for single, short term loading, and = 1.5 for a sustained load or for many cycles of repeated loading.

The average final crack spacing (in mm) for members subjected dominantly to flexure or tension can be calculated from the equation

$$s_{rm} = 50 + 0.25k_1 k_2 \phi / \rho_r$$

(6)

where ϕ is the bar size in use (or the average bar size). ρ_r is the effective reinforcement ratio, $A_s / A_{c.eff}$, where A_s is the area of reinforcement contained within the effective tension area, $A_{c.eff}$. k_1 is a coefficient which takes account of the bond properties of the bar. It is = 0.8 for high bond bars and = 1.6 for plain bond bars. k_2 is a coefficient which takes account of the strain distribution. It is = 0.5 for bending and = 1.0 for pure tension.

The crack width limit state can then be formulated by

$$g(\cdot) = w_{max} - z_c w_k$$

(7)

where z_c is a model uncertainty stochastic variable.

The stochastic variables used in the crack SLS are: concrete cover, distance between reinforcement bars, diameter of reinforcement bars, thickness of slab, elastic modulus of reinforcement bars, tensile strength of concrete, external bending moment, and one model uncertainty variable.

2.4 Deflection Limit State

The following deflection limit state is used

$$g(\cdot) = d_{max} - z_d d_k$$

(8)

3. Deterioration

3.1 Mathematical Modelling

Several models can be used to model the deterioration of reinforcement steel in concrete slabs. However, there is a general agreement that the model presented below is acceptable in most cases.

Corrosion initiation period refers to the time during which the passivation of steel is destroyed and the reinforcement starts to corrode actively. Practical experience of bridges in wetter countries like UK shows that chloride ingress is far bigger a problem that carbonation.

3

The rate of chloride penetration into concrete, as a function of depth from the concrete surface and time, can be represented by Fick's law of diffusion as follows:

$$\frac{\delta c}{\delta t} = D_C \frac{\delta^2 c}{\delta x^2} \tag{9}$$

where c is the chloride ion concentration, as % of the weight of cement, at distance x cm from the concrete surface after t seconds of exposure to the chloride source. D_C is the chloride diffusion coefficient expressed in cm^2/sec. The solution of the differential equation (8) is

$$C(x,t) = C_0 \left\{ 1 - \text{erf} \left(\frac{x}{2\sqrt{D_C t}} \right) \right\} \tag{10}$$

where C_0 is the equilibrium chloride concentration on the concrete surface, as % of the weight of cement, x is the distance from the concrete surface in cm, t is the time in sec, erf is the error function, D_C is the diffusion coefficient in cm^2/sec and $C(x,t)$ is the chloride concentration at any position x at the time t. In a real structure, if $C(x,t)$ is assumed to be the chloride corrosion threshold and x is the thickness of concrete cover, then the corrosion initiation period, T_I, can be calculated based on a knowledge of the parameters C_0 and D_C. For bridge decks under de-icing conditions $C_0=1.6$, as % of cement weight, is often used.

The time T_I to initiation of reinforcement corrosion is

$$T_I = \frac{(d_1 - D_1/2)^2}{4 D_C} \left[\text{ref}^{-1} \left(\frac{C_{cr} - C_0}{C_i - C_0} \right) \right]^{-2} \tag{11}$$

where C_i is the initial chloride concentration, C_{cr} is the critical chloride concentration at which corrosion starts, and $d_1 - D_1/2$ is the concrete cover. For plain concrete of moderate strength ($f_{cu} \approx 30 \text{ N/mm}^2$) reported values of D_C are in the range between $1 \cdot 10^{-8}$ and $5 \cdot 10^{-8}$ cm^2/sec.

When corrosion has started then the diameter $D_I(t)$ of the reinforcement bars at the time t is modelled by

$$D_I(t) = D_1 - C_{corr} i_{corr} t \tag{12}$$

where D_1 is the initial diameter, C_{corr} is a corrosion coefficient, and i_{corr} is the rate of corrosion. The area of a reinforcement bar is then modelled using the following formulation

$$A(t) = \begin{cases} n D_i^2 \frac{\pi}{4} & \text{for } t \leq T_I \\ n(D(t))^2 \frac{\pi}{4} & \text{for } T_I \leq t \leq T_I + D_i/(0.0203 \cdot i_{corr}) \\ 0 & \text{for } t > T_I + D_i/(0.0203 \cdot i_{corr}) \end{cases} \tag{13}$$

where

4

$$T_1 = \frac{x_d^2}{4D_C \left[erf^{-1}\left(\dfrac{C_{cr}(x_d,t) - C_0}{C_i - C_0} \right) \right]^2}$$

$$D t) = D_i - 0.0203(t - T_I)i_{corr\,1}$$

$A(t)$ is the area of reinforcement bars [mm^2] at the time t years, n is the number of reinforcement bars, D_i is the diameter of a single bar [mm^2] and T_I is the corrosion initiation time in years. The value "0.0203" in the estimation of $D(t)$ will vary depending on the circumstances.

The initiation time of corrosion is determined based on values of $C_0, C_i, D_C, x_d, C_{cr}$. After the deterioration is started the corrosion rate is modelled by the corrosion current i_{corr} only.
The model for $A(t)$ (and the value of i_{corr} used) relates to an average deterioration of the reinforcement in the concrete. An important aspect of corrosion in addition to the average corrosion is the maximum penetration (pitting of reinforcement). Pitting of reinforcement may have more influence on the reliability than the average deterioration due to localized much higher weakening of the reinforcement. The ratio R between the maximum penetration PC_{max} and the average penetration PC_{av} has been estimated by a number of authors to be between 4-10, see e.g. González et. al. [10]. Pitting corrosion is not included in this investigation.

The stochastic variables used in the deterioration modelling are: initial chloride concentration on surface, initial chloride concentration in concrete, diffusion coefficient for the concrete, cover to reinforcement, critical chloride concentration, and rate of corrosion.

Based on a survey the following modelling for chloride penetration is proposed (the initial chloride is assumed to be zero):

Model 0:

Diffusion coefficient $\qquad\qquad\qquad\qquad D_C:$ N(30.0, 5.0) [mm^2/year]

Chloride concentration, surface $\qquad\quad C_0:$ N(0.65, 0.075) [%]

Corrosion density $\qquad\qquad\qquad\qquad i_{corr}:$ Uniform[1.0, 3.0] [mA/cm^2]

(Cover on reinforcement $\qquad\qquad\qquad x_d:$ N(40.0, 4.0) [mm])

Figure 2 shows sample realizations of the chloride concentrations (at the depth of the reinforcement bar) for *Model 0*. Figure 3 shows sample realizations of the deterioration history of the reinforcement area for the same model.
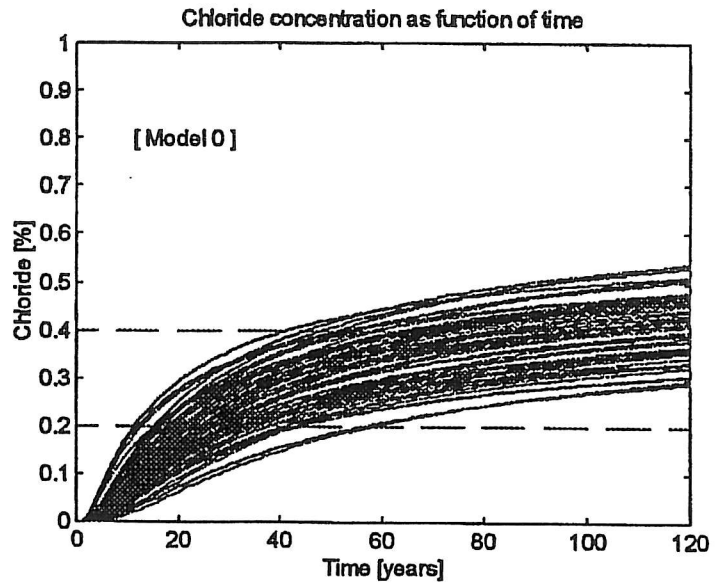
5

Figure 2. Samples showing the chloride concentration as a function of time for Model 0.
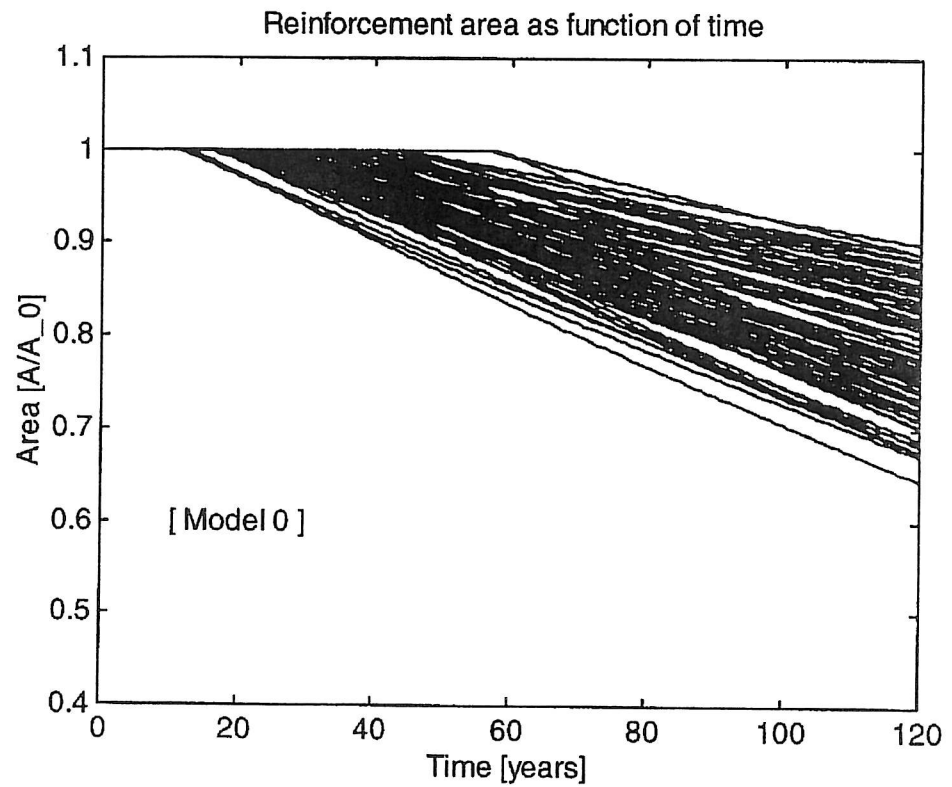

Figure 3. Normalized reinforcement area A / A_0 as a function of time for Model 0.

Based on the deterioration model 0 three levels of deterioration are proposed: low deterioration, medium deterioration and high deterioration. The deterioration parameters for these three levels are:

Low:

Diffusion coefficient	D_C:	$N(25.0, 2.5)$ [mm^2/year
Chloride concentration , surface	C_0 :	$N(0.575, 0.038)$ [%]
Corrosion density	i_{corr} :	Uniform[1.0, 2.0] [mA/cm^2

Medium:

Diffusion coefficient	D_C:	$N(30.0, 2.5)$ [mm^2/year]
Chloride concentration , surface	C_0 :	$N(0.650, 0.038)$ [%]
Corrosion density	i_{corr} :	Uniform[1.5, 2.5] [mA/cm^2

High:

Diffusion coefficient	D_C:	$N(35.0, 2.5)$ [mm^2/year
Chloride concentration , surface	C_0 :	$N(0.725, 0.038)$ [%]
Corrosion density	i_{corr} :	Uniform[2.0, 3.0] [mA/cm^2

Figure 4 shows sample realizations for the chloride concentration (at the depth of the reinforcement bar) for deterioration models: low, medium, high. The profiles obtained using mean values are shown for all three models. Figure 5 shows the sample realizations of the history of the reinforcement area for deterioration models: low, medium, high. The profiles obtained using mean values are shown for all three models .
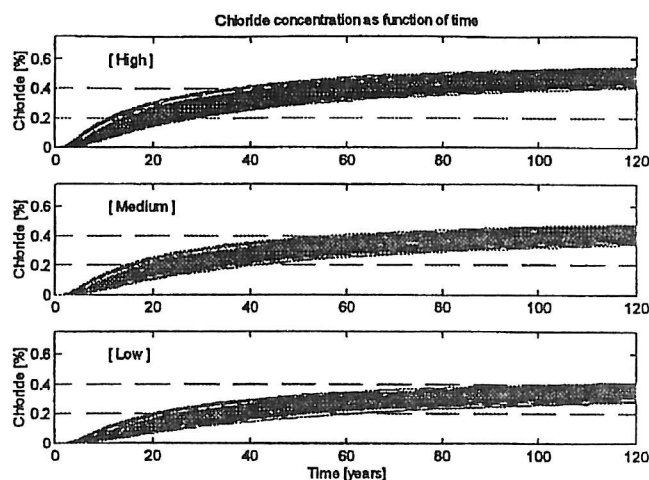

Figure 4. Samples showing the chloride concentration as a function of time for low, medium and high deterioration..
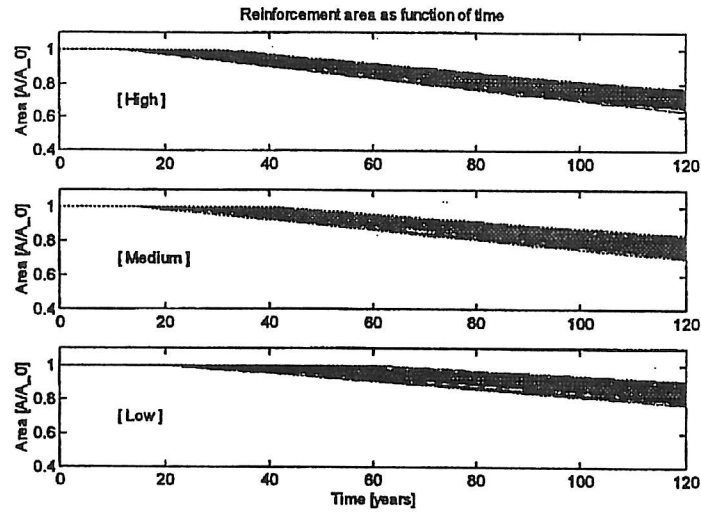
Reinforcement area as function of time

Figure 5. Normalized reinforcement area A / A_0 as a function of time for low, medium, and high deterioration..

4. Reliability Profiles

This following example is used to illustrate the proposed methodology. The example is based on an existing UK bridge, but some limitations and simplifications are made. The bridge was built in 1975.
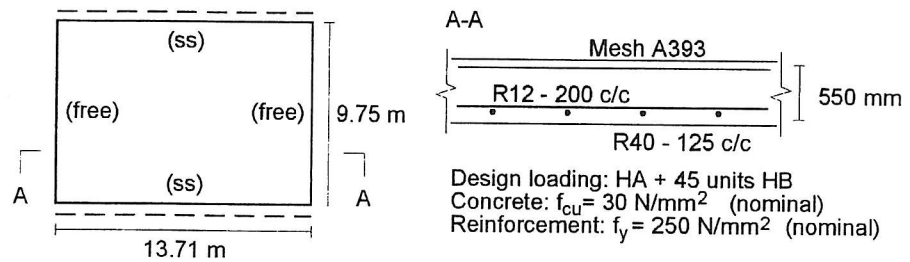

Figure 6. Bridge data.

The bridge was designed for 45 units HB load, see [10]. The bridge has a span of 9.755 m, the width is 2×13.71 m, and the slab thickness is 550 mm (see figure 6).

Based on the corrosion data shown in table 1 the expected area of the reinforcement as a function of time can be calculated, see figure 7.
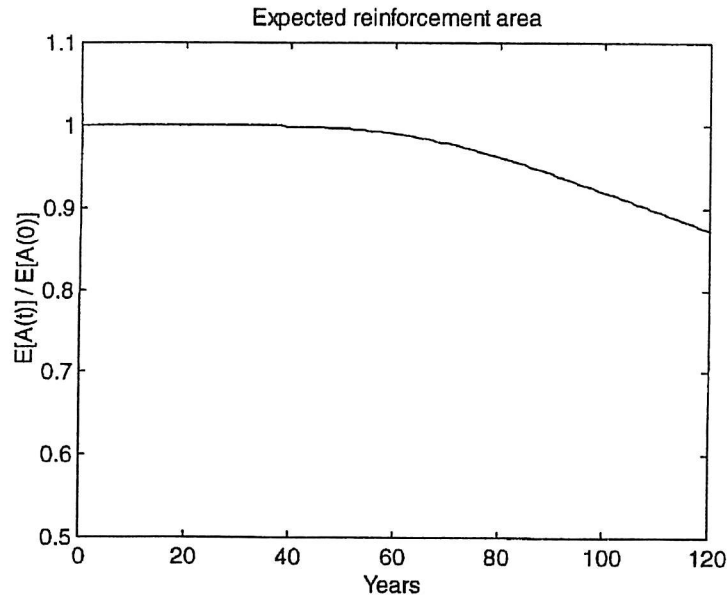
Figure 7. Reinforcement area A(t) as a function of time.

Reliability profiles for the limit states discussed in section 2 are calculated on the basis of the stochastic modelling shown in tables 1 and 2.

No	Type	Par. 1	Par. 2	Description
Stochastic variables: Yield line limit state				
1	Normal	550.0	10.0	Thickness of slab [mm]
2	LogNormal	30.0	6.0	Cube strength of concrete [MPa]
3	Normal	23.6	0.4	Density of concrete [kN/m3]
4	LogNormal	289.0	25.0	Yield strength: longitudinal reinforcement [MPa]
5	Normal	60.0	8.0	Cover on longitudinal reinforcement [mm]
6	LogNormal	289.0	25.0	Yield strength: transverse reinforcement [MPa]
7	Normal	86.0	8.0	Cover on transverse reinforcement [mm]
8	Fixed	10053.0	-	Longitudinal reinforcement area (initial) [mm2]
9	Fixed	565.0	-	Transverse reinforcement area (initial) [mm2]
10	Gumbel	0.352	0.026	Static load factor [-]
11	Normal	1.27	0.20	Dynamic load factor [-]
12	Normal	1.08	0.072	Chloride concentration on surface [%]
13	Fixed	0.0	-	Initial chloride concentration [%]
14	Normal	35.0	2.5	Diffusion Coefficient [cm2/sec]
15	Normal	0.4	0.05	Critical Chloride concentration [%]
16	Uniform	2.5	0.29	Corrosion parameter [-]
17	Normal	1.0	0.05	Model uncertainty variable [-]

Table 1. Stochastic modelling used for the ULS.

Stochastic variables: Crack width limit state				
No	Type	Par. 1	Par. 2	Description
1	Normal	60.0	9.0	Concrete cover [mm]
2	Normal	125.0	12.5	Distance between reinforcement bars [mm]
3	Normal	40.0	1.2	Diameter of reinforcement bar [mm]
4	Normal	550.0	27.0	Thickness of slab [mm]
5	Normal	200.0E3	6.0E3	Young's modulus [N/mm2]
6	Normal	3.4	0.68	Tensile strength [N/mm2]
7	Gumbel	1.0	0.10	Model uncertainty [-]
8	Gumbel	0.352	0.026	Static load factor [-]
9	Normal	1.27	0.20	Dynamic load factor [-]
10	Normal	1.08	0.072	Chloride concentration on surface [%]
11	Fixed	0.0	-	Initial chloride concentration [%]
12	Normal	35.0	2.5	Diffusion Coefficient [cm2/sec]
13	Normal	0.4	0.05	Critical Chloride concentration [%]
14	Uniform	2.5	0.29	Corrosion parameters [-]

Table 2. Stochastic modelling used for the SLS.

The general traffic highway load model in the Eurocode 1, Part 3 (ENV 1991-3:1995) for lane and axle load is applied. The load effects produced by the Eurocode model (lane and axle load) are multiplied by a static load factor (extreme type 1) and a dynamic load factor (normal).

The normalized reliability profile for the yield line ULS (full width failure) and the corresponding probability of failure profile are shown in figure 8. The reliability index at time $t = 0$ is $\beta_0 = 11.5$. Due to the size of the concrete cover (mean value 60 mm) the deterioration does not have any effect until year 70.
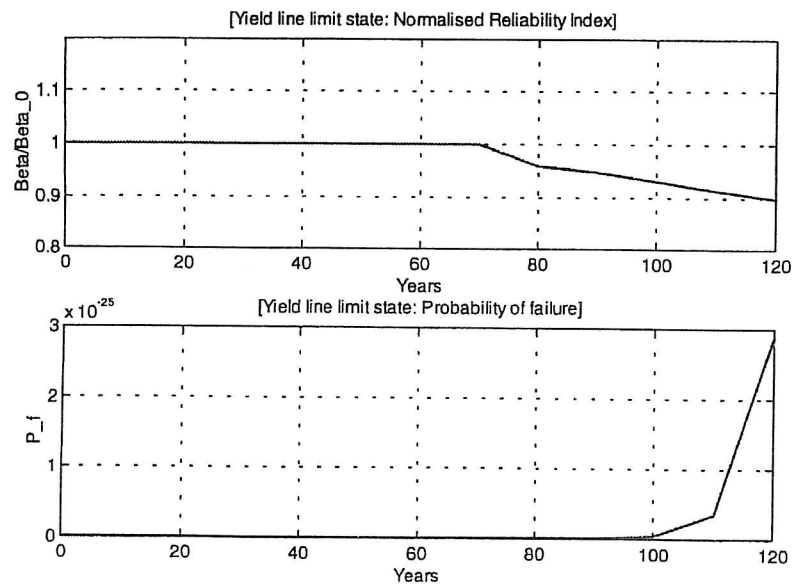

Figure 8. : Reliability profiles using a yield line limit state.

The results from the sensitivity analysis with regard to the mean values are shown for t=0 years and $t = 120$ years in figure 9. The most important variables are, as expected, the thickness of the slab, the yield strength of the reinforcement, and the model uncertainty. Observe that the magnitude of sensitivity with regard to the cover changes from negative at the time $t = 0$ to positive at the time $t = 120$ due to the corrosion.
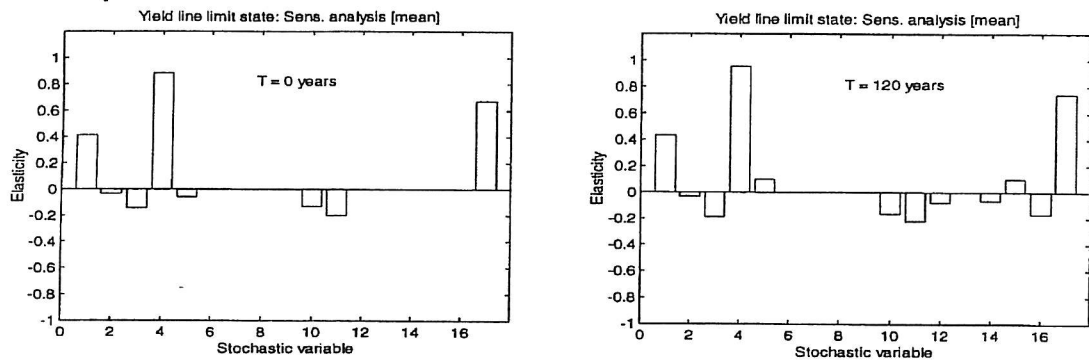

Figure 9 : Sensitivity analysis for yield line limit state at $t = 0$ years and at $t = 120$ years.

The normalized reliability profile for the crack SLS and the corresponding probability of failure profile are shown in figure 10. The reliability index at time $t = 0$ is $\beta_0 = 7.1$. Due to the size of the concrete cover (mean value 60 mm) the deterioration does not have any effect until year 90.
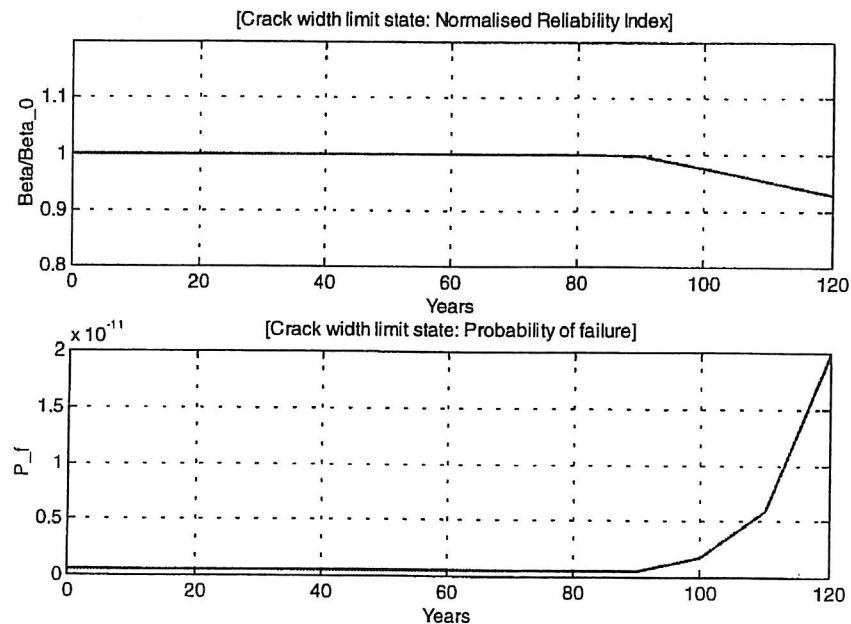

Figure 10 : Reliability profiles using a crack width limit state

The results from the sensitivity analysis with regard to the mean values are shown for $t = 0$ years and $t = 120$ years in figure 11. The most important variables are as expected the concrete cover, the diameter of the reinforcement, the thickness of the slab, and Young's modulus.

Observe that the magnitude of the sensitivity with regard to the cover is decreasing from time $t = 0$ to the time $t = 120$ due to the corrosion.
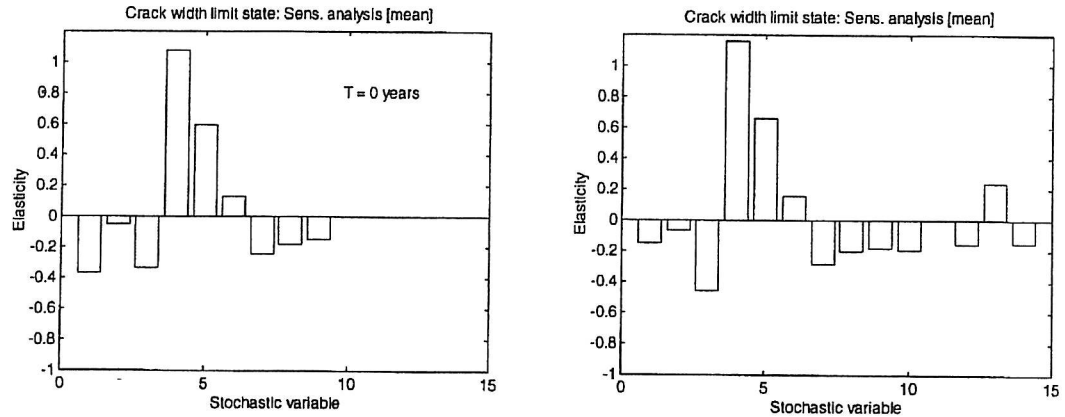

Figure 11. Sensitivity analysis for crack width limit state at $t = 0$ years and $t = 120$ years.

5. K factor Profiles

In this section a new procedure is proposed for use by engineers when assessing bridges.

For a given bridge, using the loading given in the Assessment Code BD21, the available load capacity factor, K, is initially calculated. A chart like Fig. 12 is supplied to the assessing engineer. If the calculated K factor is below the indicated safety level then immediate action is required (e.g. strengthening, repair or replacement).

If the load capacity factor K is above the lines (b), (c) or (d), corresponding to the road being a trunk road, a principal road or a minor road, or line (e) (shown schematically in Fig. 12), then the bridge can be deemed satisfactory and no strengthening work is necessary at present.

If the load capacity factor K is within the intermediate zone (the safety line and lines (b), (c), (d) or (e)), the assessing engineer is required to determine all reasonable alternative strengthening/repair/maintenance strategies for the bridge. These data and alternatives are then made available to the owner/maintainer of the bridge who then decides which actions to take.
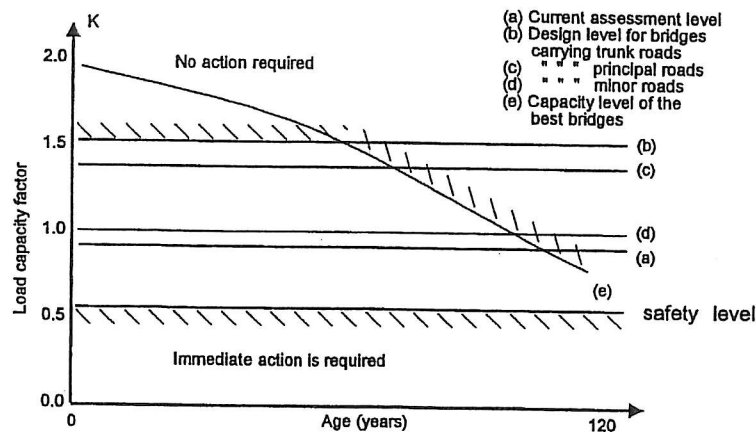
Figure 12. typical form of local capacity factor chart.

6. Acknowledgement

7. References

[1] Thoft-Christensen, P. , F.M.Jensen, C.Middleton & A.Blackmore: "*Assessment of the Reliability of Concrete Slab Bridges*". IFIP WG7.5 Conference, Boulder, USA, April 2-4, 1996.

[2] Thoft-Christensen, P.: "*Re-Assessment of Concrete Bridges*". ASCE Structures Congress, Chicago, USA, April 14-18, 1996

[3] Middleton, C. Example Collapse & Reliability Analyses of Concrete Bridges Using a new Analyses Technique. Cambridge University, 1994.

[4] RELIAB01, Version 2.0 , manual and software. CSR-software, March 1994.

[5] RELIAB02, Version 2.0 , manual and software. CSR-software, April 1994.

[6] P. Thoft-Christensen: "*Reliability of Plastic Slabs*", ICOSSAR Conference, San Francisco, USA, August 1989.

[7] CORROSION, Version 1.0 , manual and software. CSR-software, September 1995.

[8] Eurocode 2: Design of concrete structures - Part 1-1: General rules and rules for buildings, ENV 1992-1:1991.

[9] J .A. González, C. Andrade, C. Alonso & S. Feliu: "*Comparison of Rates of General Corrosion and Maximum Pitting Penetration on Concrete Embedded Steel Reinforcement*", Cement and Concrete Research, Vol. 25, No. 2, pp. 257-264, 1995.

[10] Department of Transport. Loads for Highway Bridges. Departmental Standard BD37/88, London, 1989.

STRUCTURAL RELIABILITY THEORY SERIES

PAPER NO. 144: S. Engelund: *Probabilistic Models and Computational Methods for Chloride Ingress in Concrete.* Ph.D.-Thesis. ISSN 1395-7953 R9707.

PAPER NO. 145: H. U. Köylüoğlu, S. R. K. Nielsen, Jamison Abbott & A. Ş. Çakmak: *Local and Modal Damage Indicators for Reinforced Concrete Shear Frames subject to Earthquakes.* ISSN 0902-7513 R9521

PAPER NO. 146: P. H. Kirkegaard, S. R. K. Nielsen, R. C. Micaletti & A. Ş. Çakmak: *Identification of a Maximum Softening Damage Indicator of RC-Structures using Time-Frequency Techniques.* ISSN 0902-7513 R9522.

PAPER NO. 147: R. C. Micaletti, A. Ş. Çakmak, S. R. K. Nielsen & P. H. Kirkegaard: *Construction of Time-Dependent Spectra using Wavelet Analysis for Determination of Global Damage.* ISSN 0902-7513 R9517.

PAPER NO. 148: H. U. Köylüoğlu, S. R. K. Nielsen & A. Ş. Çakmak: *Hysteretic MDOF Model to Quantify Damage for TC Shear Frames subject to Earthquakes.* ISSN 1395-7953 R9601.

PAPER NO. 149: P. S. Skjærbæk, S. R. K. Nielsen & A. Ş. Çakmak: *Damage Location of Severely Damaged RC-Structures based on Measured Eigenperiods from a Single Response.* ISSN 0902-7513 R9518.

PAPER NO. 150: S. R. K. Nielsen & H. U. Köylüoğlu: *Path Integration applied to Structural Systems with Uncertain Properties.* ISSN 1395-7953 R9602.

PAPER NO. 151: H. U. Köylüoğlu & S. R. K. Nielsen: *System Dynamics and Modified Cumulant Neglect Closure Schemes.* ISSN 1395-7953 R9603.

PAPER NO. 152: R. C. Micaletti, A. Ş. Çakmak, S. R. K. Nielsen, H. U. Köylüoğlu: *Approximate Analytical Solution for the 2nd-Order moments of a SDOF Hysteretic Oscillator with Low Yield Levels Excited by Stationary Gaussian White Noise.* ISSN 1395-7953 R9715.

PAPER NO. 153: R. C. Micaletti, A. Ş. Çakmak, S. R. K. Nielsen & H. U. Köylüoğlu: *A Solution Method for Linear and Geometrically Nonlinear MDOF Systems with Random Properties subject to Random Excitation.* ISSN 1395-7953 R9632.

PAPER NO. 154: J. D. Sørensen, M. H. Faber, I. B. Kroon: *Optimal Reliability-Based Planning of Experiments for POD Curves.* ISSN 1395-7953 R9542.

PAPER NO. 155: J. D. Sørensen, S. Engelund: *Stochastic Finite Elements in Reliability-Based Structural Optimization.* ISSN 1395-7953 R9543.

PAPER NO. 156: C. Pedersen, P. Thoft-Christensen: *Guidelines for Interactive Reliability-Based Structural Optimization using Quasi-Newton Algorithms.* ISSN 1395-7953 R9615.

PAPER NO. 157: P. Thoft-Christensen, F. M. Jensen, C. R. Middleton, A. Blackmore: *Assessment of the Reliability of Concrete Slab Bridges.* ISSN 1395-7953 R9616.

PAPER NO. 158: P. Thoft-Christensen: *Re-Assessment of Concrete Bridges.* ISSN 1395-7953 R9605.

STRUCTURAL RELIABILITY THEORY SERIES

PAPER NO. 159: H. I. Hansen, P. Thoft-Christensen: *Wind Tunnel Testing of Active Control System for Bridges.* ISSN 1395-7953 R9662.

PAPER NO 160: C. Pedersen: *Interactive Reliability-Based Optimization of Structural Systems.* Ph.D.-Thesis. ISSN 1395-7953 R9638.

PAPER NO. 161: S. Engelund, J. D. Sørensen: *Stochastic Models for Chloride-initiated Corrosion in Reinforced Concrete.* ISSN 1395-7953 R9608.

PAPER NO. 162: P. Thoft-Christensen, A. S. Nowak: *Principles of Bridge Reliability - Application to Design and Assessment Codes.* ISSN 1395-7953 R9751.

PAPER NO. 163: P. Thoft-Christensen, F.M. Jensen, C. Middleton, A. Blackmore: *Revised Rules for Concrete Bridges.* ISSN 1395-7953 R9752.

PAPER NO. 164: P. Thoft-Christensen: *Bridge Management Systems. Present and Future.* ISSN 1395-7953 R9711.

PAPER NO. 165: P. H. Kirkegaard, F. M. Jensen, P. Thoft-Christensen: *Modelling of Surface Ships using Artificial Neural Networks.* ISSN 1593-7953 R9625.

PAPER NO. 166: S. R. K. Nielsen, S. Krenk: *Stochastic Response of Energy Balanced Model for Wortex-Induced Vibration.* ISSN 1395-7953 R9710.

PAPER NO. 167: S.R.K. Nielsen, R. Iwankiewicz: *Dynamic systems Driven by Non-Poissonian Impulses: Markov Vector Approach.* ISSN 1395-7953 R9705.

PAPER NO. 168: P. Thoft-Christensen: *Lifetime Reliability Assessment of Concrete Slab Bridges.* ISSN 1395-7953 R9717.

PAPER NO. 169: P. H. Kirkegaard, S. R. K. Nielsen, I. Enevoldsen: *Heavy Vehicles on Minor Highway Bridges - A Literature Review.* ISSN 1395-7953 R9719.

PAPER NO. 170: S.R.K. Nielsen, P.H. Kirkegaard, I. Enevoldsen: *Heavy Vehicles on Minor Highway Bridges - Stochastic Modelling of Surface Irregularities.* ISSN 1395-7953 R9720.

PAPER NO. 171: P. H. Kirkegaard, S. R. K. Nielsen, I. Enevoldsen: *Heavy Vehicles on Minor Highway Bridges - Dynamic Modelling of Vehicles and Bridges.* ISSN 1395-7953 R9721.

PAPER NO. 172: P. H. Kirkegaard, S. R. K. Nielsen, I. Enevoldsen: *Heavy Vehicles on Minor Highway Bridges - Calculation of Dynamic Impact Factors from Selected Crossing Scenarios.* ISSN 1395-7953 R9722.

PAPER NO. 175: C. Frier, J.D. Sørensen: *Stochastic Properties of Plasticity Based Constitutive Law for Concrete.* ISSN 1395-7953 R9727.

PAPER NO. 177: P. Thoft-Christensen: *Review of Industrial Applications of Structural Reliability Theory.* ISSN 1395-7953 R9750.